JVI Journals.ASM.org

Four Amino Acids of an Insect Densovirus Capsid Determine Midgut Tropism and Virulence

Cecilia Multeau,[a,b,c] Rémy Froissart,[d,e] Aurélie Perrin,[a,b] Ilaria Castelli,[f] Morena Casartelli,[f] and Mylène Ogliastro[b,c]

Invivo AgroSolutions, Valbonne, France[a]; INRA, UMR 1333 DGIMI, INRA, Montpellier, France[b]; Université Montpellier 2, Montpellier, France[c]; CNRS, UMR 5290 MIVEGEC, Montpellier, France[d]; CIRAD-SupAgro, UMR 385 BGPI, Montpellier, France[e]; and Dipartimento di Biologia, Università degli Studi di Milano, Milan, Italy[f]

Densoviruses are insect parvoviruses that are orally infectious for *Lepidoptera*. To assess the mechanisms underlying their specificity and their virulence, we investigated the role of eight candidate residues in the densovirus capsid. We showed that the substitutions of four amino acids were associated with decreased virulence due to a decreased ability to cross the host midgut epithelium, without an effect on viral replication in other tissues.

Densoviruses are arthropod parvoviruses (classified as *Densovirinae*) characterized by a nonenveloped capsid protecting a short single-stranded DNA genome. Their pathogenicity for insects at larval stages suggests that they could be interesting agents for the control of insect populations, provided that their potential unwanted side effects on nontargeted populations are understood.

Densovirinae display a great diversity in structure, sequence, and host range. There are four known genera; the genus *Densovirus* (DNV) infects exclusively *Lepidoptera* (14). According to the International Committee on Taxonomy of Viruses (ICTV), two viruses have been classified so far in this genus: the type species *Junonia coenia* DNV (*Jc*DNV) and the greater wax moth *Galleria mellonella* DNV (*Gm*DNV). They are characterized by ambisense genomes displaying 88% sequence identity. They infect similar tissues in their hosts, both excluding the midgut, but differ in their host range. *Jc*DNV infects several lepidopteran species but not *G. mellonella*, while *Gm*DNV appears restricted to this host.

DNVs are orally transmitted. Once ingested by the larvae, viral particles must cross the intestinal barrier of their host to reach and replicate in the underlying target tissues (12). The host digestive tract, and particularly the entry in the epithelial cells of the midgut, is the first step that determines specificity.

Parvovirus capsids are icosahedral with a T=1 symmetry, and the surface is shaped by 60 copies of a common core of structural proteins (VP) (4). Substitutions on the surfaces of vertebrate parvovirus capsids have been associated with changes in tissue tropism and host shift (7, 8, 10). Four proteins sharing a common C terminus and extended N termini compose the DNV capsid (VP1 to -4), displaying 88% sequence identity. They are translated at different ratios by a leaky scanning mechanism; VP4, the most abundant VP, shapes the surface of the capsid. The VP4s of *Gm*- and *Jc*DNV are each made of 437 amino acids (aa) and display 96% sequence identity.

The molecular anatomy of several parvoviruses has been solved by X-ray crystallography and cryo-electron microscopy (cryo-EM), which elucidate the early mechanisms of specificity (3). The molecular mechanisms driving DNV's specificity are currently unknown, and no cellular receptors have been characterized so far. The structure of *Gm*- and *Jc*DNV has been solved by X-ray crystallography and cryo-EM, respectively (2, 13). They share with vertebrate parvoviruses a highly conserved beta barrel core, although their surface is smoother, with only two small reliefs in the 5-fold axis and none of the prominent spike on the 3-fold axis shown to be involved in the parvovirus attachment to the receptor (8).

By comparing the VP4s of *Gm*- and *Jc*DNV, Bruemmer et al. identified 22 differences in amino acids, of which 8 aa are exposed at the surface and may act as potential determinants of host specificity (2). Five of these differences are located on the two unique reliefs on the 5-fold axis: two at the tip and the base of the smaller spike (at positions 177 and 174, respectively), and three around the larger spike (positions 167, 276, and 196) (Fig. 1). The last 3 aa changes were located close to the 5-fold axis (position 123), in the 3-fold axis (position 297), and in a dimple on the 2-fold axis (position 305) (2). By analogy with parvovirus data, the two small reliefs on the 5-fold axis in DNV capsid have been considered the strongest candidates for host range or tropism (2, 7, 8, 10, 13).

Based on these structural data, we produced eight mutants of *Jc*DNV by substituting at these sites the *Gm*DNV amino acids. We then characterized *in vivo* the role of these residues on virulence. The results presented here provide functional insight *in insecta* on densovirus determinants of virulence and tissue specificity.

A *Jc*DNV mutant harboring *Gm*DNV amino acids has a reduced virulence in the *Spodoptera frugiperda* host. To construct *Jc*DNV mutant viruses, site-directed mutagenesis was carried out to replace VP4 candidate residues with those of *Gm*DNV. Substitutions were carried out in an infectious molecular clone of the *Jc*DNV wild-type (wt-*Jc*DNV) genome, pBRJH (9). In total, eight *Jc*DNV mutants (m-*Jc*DNVs) were constructed: six mutants carried a single substitution (A123V, S167T, A196T, A276V, I297T, or S305N), one mutant combined two close substitutions in the strongest candidate relief (I174V/T177D), and one mutant carried all the substitutions (8m) (Table 1). Transfecting mutants and wt pBRJH in *S. frugiperda* larvae generated all viral stocks, which were subsequently purified and quantified by quantitative PCR (qPCR). The proper assembly of the viral particles was analyzed by electron microscopy, and the presence of mutations confirmed by

Received 17 November 2011 **Accepted** 22 February 2012
Published ahead of print 29 February 2012
Address correspondence to Mylène Ogliastro, ogliastr@supagro.inra.fr.

doi:10.1128/JVI.06839-11

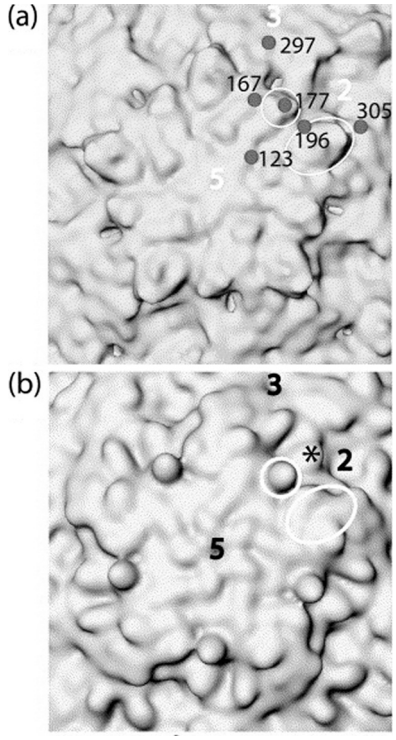

FIG 1 Close-up view along the 5-fold axis of (a) *Jc*DNV and (b) *Gm*DNV. An example of the smaller spike is marked with a circle, and an example of the second spike is marked with an oval in each panel. In panel b, an asterisk marks the small protuberance near the 2-fold axis that is present on *Gm*DNV but not *Jc*DNV (kindly provided by A. Bruemmer).

sequencing the viral genomes before and after their amplification in larvae.

We first estimated the virulence by assessing the time to death and the mortality of larvae induced by these viruses. Cohorts of 30-s instar *S. frugiperda* larvae were infected with wt-*Jc*DNV and all m-*Jc*DNVs at two viral doses, 1E+06 and 1E+08 viral equivalent genomes (veg) per larva. These doses were previously determined by qPCR to correspond, respectively, to wt-*Jc*DNV doses killing 50% and 95% of a larval cohort (LD_{50} and LD_{95}, respectively). Virulence was assessed until death or nymphosis (15 days). Infections were similarly performed with cohorts of *G. mellonella* larvae.

Caterpillars infected with A123V, I174V/T177T, and 8m mutants displayed a higher survival rate at both doses ($P < 0.001$; Dunnett test) compared to those infected with wt-*Jc*DNV, suggesting a lower virulence of these mutants (Fig. 2A). Virulence was intermediate for the S167T mutant, i.e., similar at LD_{95} but lower at LD_{50} (P values of 0.29 and <0.01, respectively; Dunnett test), while no difference in virulence was observed for the A196T, A276V, I297T, and S305N mutants. The time to death was delayed in *S. frugiperda*, the strongest effect was observed for infections with mutant 8m. At LD_{50}, almost all 8m-infected larvae went through nymphosis within 2 weeks (Fig. 2B). Increasing the dose to LD_{95} delayed the death of 8m-infected larvae by 6 to 7 days compared to controls (data not shown).

No mortality of *G. mellonella* larvae was observed, even at an over-lethal dose (1E+11 veg/larva), showing that these residues are not sufficient to exchange virus specificity.

We next sought to determine whether the stability of the capsid was affected by mutations. In the route of infection, viral particles cross a wide range of pHs, from highly basic (pH 9 to 10) in the gut of phytophagous caterpillars to acidic (pH 4 to 5) in endosomal compartments. Such environments could negatively affect the stability of potentially weakened mutant capsids. To test this hypothesis, we challenged 8m and wt particles at pH 9 for 1 h prior to oral infections of *S. frugiperda* larvae and compared the resulting virulence by determining the LD_{50}s. The pH 9 challenge did not significantly affect the LD_{50}s.

By analogy with parvoviruses, mutations in or near the 5-fold axis might be detrimental for infectivity, impairing for example the externalization of VP1 during the traffic toward the nucleus (1, 5). To assess this point, we determined the infectivity of all viruses *in vitro* using the Ld652 permissive cell line (9, 14). Infectious titers on these cells were all similar, further suggesting that viral structures were not compromised by the mutations (11, 16). No loss in virulence was observed either by challenging viral particles to a high temperature (up to 50°C for 1 h) before ingestion.

The loss in virulence is thus unlikely to result from an altered stability of the mutated capsid in the course of infection.

To quantify the loss in virulence, we next determined the LD_{50} and LD_{95} for the four mutants by infecting 30 larvae with serial viral dilutions. The A196T mutant, referred to as a "neutral" mutant, and wt-*Jc*DNV were included as controls. As shown on Fig. 2C, a 10- to 1,000-fold increase in LD_{50} and LD_{95} was obtained depending on the virus, and the strongest effect was again observed for the 8m mutant carrying all aa substitutions. No difference was observed between the two controls.

The results showed that four of the eight predicted residues located on or near the 5-fold axis protrusions are important for *Jc*DNV virulence, but not stability, in *S. frugiperda*. We next enquired which step in the infection process was affected.

Substitutions on *Jc*DNV capsid do not affect replication within target cells. We first analyzed the tissue tropism. Larvae were infected with mutants and wt-*Jc*DNV at their respective LD_{95}s (Fig. 2C); tissue tropism was assessed for dying larvae by immune-labeling as previously described (12). Viruses were antigenically cross-reactive, and a similar tissue tropism was observed for all the mutants tested (data not shown). The low virulence of the 8m mutant was thus not due to a change in tissue tropism.

We next quantified with time the replication of m- and wt-*Jc*DNV in the larvae. Previous work carefully dissected the *Jc*DNV pathogenesis in *S. frugiperda* (12). These studies revealed that viral

TABLE 1 Candidate amino acid positions and localization on VP4 capsid surface proteins[a]

Localization on VP4 aa sequence	Localization on the capsid surface	*Jc*DNV residue	*Gm*DNV residue
123	5-Fold axis	A	V
167	Base large peak	S	T
174	Base small peak	I	V
177	Top small peak	T	D
196	Close large peak	A	T
276	Base large peak	A	V
297	3-Fold axis	I	T
305	Dimple 2-fold axis	S	N

[a] Shown are candidate aa positions and localization on *Gm*DNV and *Jc*DNV VP4 capsid surface proteins NC_004286 and NC_004284, respectively.

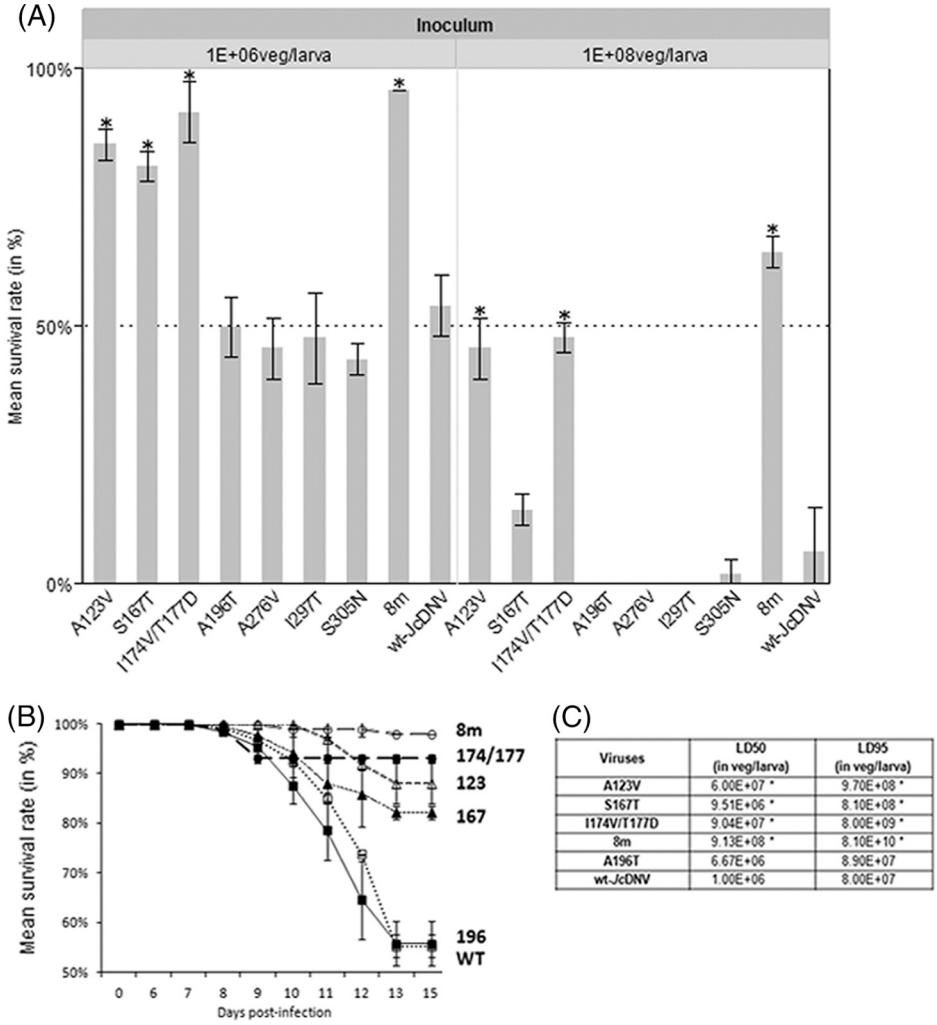

Viruses	LD50 (in veg/larva)	LD95 (in veg/larva)
A123V	6.00E+07 *	9.70E+08 *
S167T	9.51E+06 *	8.10E+08 *
I174V/T177D	9.04E+07 *	8.00E+09 *
8m	9.13E+08 *	8.10E+10 *
A196T	6.67E+06	8.90E+07
wt-JcDNV	1.00E+06	8.00E+07

FIG 2 Specific amino acid substitutions on the *Jc*DNV capsid surface affect virulence on *S. frugiperda* larvae. (A) Mean larval survival rates following infections with m- or wt-*Jc*DNV at the LD_{50} and the LD_{95} of wt-*Jc*DNV (1E+06 and 1E+08 veg/larva, respectively). Survival was assessed until death or nymphosis (15 days). (B) Kinetic of mean larval survival rates following infections with m- or wt-*Jc*DNV at the LD_{50} of wt-*Jc*DNV (1E+06 veg/larva). (C) m- and wt-*Jc*DNV LD_{50} and LD_{95} calculated by serial dilutions. Asterisks indicate results statistically different from those for wt-*Jc*DNV using Dunnett tests with wt-*Jc*DNV as the control.

replication is not observed in midgut cells and is restricted to underlying target tissues, e.g., visceral muscles and trachea, where a viral clearance and a phase of viral eclipse follow entry (12). Further, at day 2 postinfection (p.i.), the input virus is entirely eliminated and replication is barely detected in target tissues. By this time, infectious viruses have crossed the midgut.

To compare viral loads between viruses, cohorts of 50 larvae were infected with 1E+09 and 1E+11 veg/larva (respectively, the LD_{50} and LD_{95} rounded values of the less-virulent mutant, 8m). Next, four larvae per virus and per dose were sacrificed every day. Viral loads per larva were estimated by qPCR as previously described (12). At day 2 p.i. and at both doses, viral loads were significantly lower in larvae infected with m-*Jc*DNVs than those in controls ($P < 0.05$; Dunnett test), suggesting a decreased midgut crossing. Similar loads were recovered with time for mutants A123V, S167T, and I174V/T177T and controls ($P > 0.85$; Dunnett test) (Fig. 3). Larvae infected with the 8m mutant were the only ones still displaying lower viral loads at 10 days p.i. ($P < 0.05$), although few dead larvae were observed. Similar values were calculated for the slope of viral accumulation curves (data not shown) suggesting that the abilities of all viruses to replicate in target tissues are similar. Infection for mutant viruses might then be delayed as a matter of dose at the early step of viral entry. Mutations might affect the capacity of the virus to reach the target tissues by limiting its capacity to cross the midgut.

Four aa on *Jc*DNV capsid define the efficiency of midgut crossing. If mutations affect the midgut crossing, then virulence should be similar for infections bypassing the midgut, i.e., by direct virus injections in the larval haemocoel. To test this hypothesis, we first determined the LD_{50} and LD_{95} by injecting 4th instar *S. frugiperda* larvae with serial dilutions of m- and wt-*Jc*DNV. The LDs of all m-*Jc*DNV*s* were similar to those of the controls, wt-*Jc*DNV and mutant A196T ($P > 0.41$) (Fig. 4A). As hypothesized, no loss in virulence was observed when the midgut was bypassed, strongly suggesting that capsid substitutions affect the midgut tropism. No mortality was observed following the injection of mutants in *G. mellonella*.

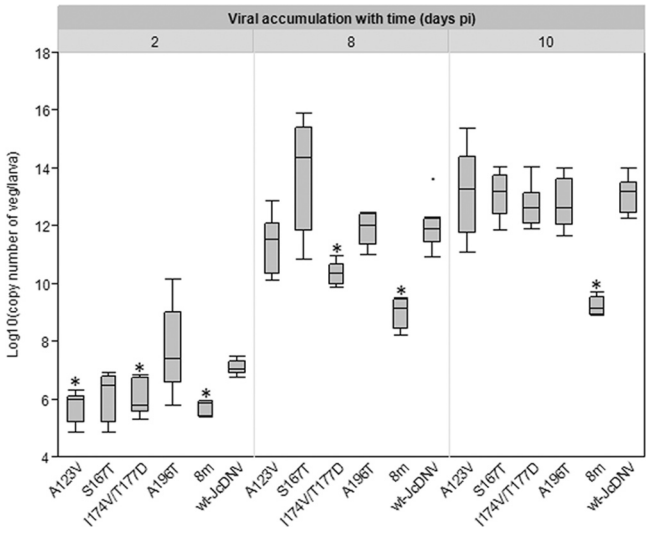

FIG 3 The A123V, S167T, I174V/T177D, and 8m mutant viruses efficiently replicate in *S. frugiperda* larvae. Larvae were infected at the LD_{50} of the mutant with the lowest virulence, the 8m mutant (1E+09 veg/larva). Results are presented as $\log_{10}$(copy number of veg/larva). Asterisks indicate results statistically different from those for wt-*Jc*DNV using Dunnett tests with wt-*Jc*DNV as the control.

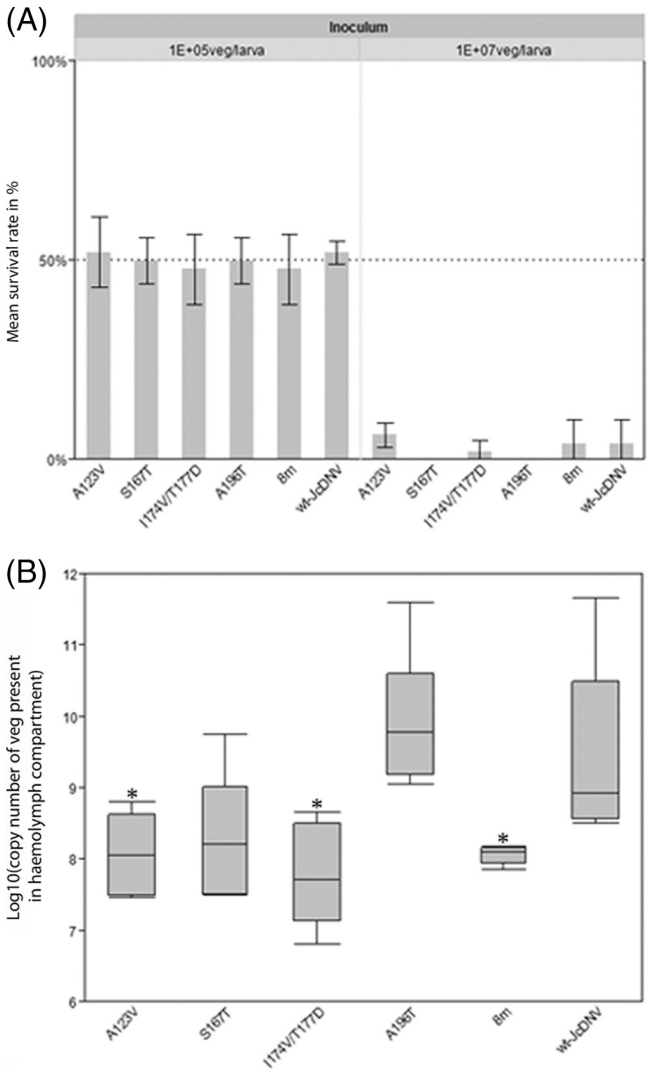

FIG 4 The A123V, S167T, I174V/T177D, and 8m mutant viruses have a decreased capacity to cross the midgut of *S. frugiperda* larvae compared to that of wt-*Jc*DNV. (A) Larval survival rates 15 days following injections with m- or wt-*Jc*DNV at the LD_{50} and the LD_{95} of injected wt-*Jc*DNV (1E+05 and 1E+07 veg/larva, respectively). No significant difference was obtained for m-*Jc*DNV compared to wt-*Jc*DNV. (B) *Ex vivo* analysis of the capacities of m- and wt-*Jc*DNV to cross the *S. frugiperda* midgut. Asterisks indicate results statistically different from those for wt-*Jc*DNV (Dunnett tests with wt-*Jc*DNV as the control).

To underpin this hypothesis, we next measured the ability of viruses to cross the midgut of *S. frugiperda ex vivo*, using Ussing chambers. This device allowed to isolate the luminal (L) from the hemolymphatic (H) sides of an epithelium and study the trafficking of macromolecular complexes or ions (15). The Ussing chambers have been successfully adapted to large lepidopteran midgut epithelium, including *S. frugiperda* but not *G. mellonella*, which is too small to be mounted (6). In this setting, tissue integrity is retained for 2 to 3 h as measured by the transepithelial resistance assessing the permeability of the tissues. Midguts of *S. frugiperda* 6th instar larvae were dissected and opened to produce a single layer, which was mounted in between the two chambers as previously described (6). After a 30-min equilibration, m- or wt-*Jc*DNV (1E+13 veg) were added to the L compartment and left for 30 min. The total volume of both compartments (500 μl each) was then recovered separately to extract DNA and estimate the amount of viral genomes by qPCR. At least six repeats on different midguts were performed for each virus. The total amount of DNA recovered from both compartments (L and H) was similar between experiments and between viruses ($P > 0.76$). The ratio of the number of wt viral genomes that crossed the midgut, over the total amount of input viral genomes was about 1 in 1E+04 during the 30 min that the experiment lasts (Fig. 4B). The amounts of m-*Jc*DNV crossing the midgut were significantly lower for the A123V, I174V/T177T, and 8m viruses compared to those for the controls ($P < 0.05$; Dunnett test). These results further confirmed that substitutions on residues located near or at the 5-fold axis protrusion affected the capacity of *Jc*DNV to reach the haemocoel. Results obtained for the S167T mutant were always statistically less significant than those with the A123V and I174V/T177T mutants, suggesting a more minor role of this residue when alone and/or a potentiating role when combined with the three other residues. Altogether, our results provide the first functional data (both *in vivo* and *ex vivo*) on densovirus virulence and midgut tropism determinants on the capsid. Four of the eight residues structurally predicted to be involved in host specificity significantly affect virulence upon ingestion by *S. frugiperda* larvae. Their substitutions markedly decrease the number of viral particles crossing the midgut but do not appear to affect replication once this barrier is overcome, clearly indicating that these four residues are involved in midgut tropism. The mutated capsids may have a lower affinity for midgut-specific molecules involved in recognition and/or entry of the viral particles; we are currently investigating the mechanism of midgut crossing. These results suggest that two different mechanisms control tissue specificity, one for midgut entry and one for target tissues entry and replication.

This study highlights the great potential of the densovirus/*Lepidoptera* interaction model and the suitability of virus chimeras for *in vivo* mechanistic studies on virulence and specificity.

ACKNOWLEDGMENTS

We warmly thank C. Gibard, M. Jambart, and G. Clabot for animal husbandry and providing collections of larvae, M. Ravallec for TEM observations. Special thanks go to E. Jacox for his very helpful English assistance and to C. Dumas for his critical comments. We also wish to thank P. Clair from the Montpellier GenomiX qPCR facility of the University Montpellier II and the TEM facility (UM2, Montpellier) for their technical support. We are infinitely grateful to A. Bruemmer for kindly providing the figure pointing key amino acids at the surface of the capsid of *Jc*DNV.

This work was supported by a CIFRE Ph.D. fellowship from the French Association Nationale Recherche Technologie, *In vivo* AgroSolutions from the Union *In vivo* group, and the French Institut National de la Recherche Agronomique.

REFERENCES

1. **Bleker S, Sonntag F, Kleinschmidt JA.** 2005. Mutational analysis of narrow pores at the fivefold symmetry axes of adeno-associated virus type 2 capsids reveals a dual role in genome packaging and activation of phospholipase A2 activity. J. Virol. **79**:2528–2540.
2. **Bruemmer A, Scholari F, Lopez-Ferber M, Conway JF, Hewat EA.** 2005. Structure of an insect parvovirus (Junonia coenia Densovirus) determined by cryo-electron microscopy. J. Mol. Biol. **347**:791–801.
3. **Chapman MS, Agbandje-McKenna M.** 2006. Atomic structure of viral particles, p 109–123. *In* Bloom ME, et al (ed), Parvoviruses. Edward Arnold, London, United Kingdom.
4. **Cotmore SF, Tattersall P.** 2007. Parvoviral host range and cell entry mechanisms. Adv. Virus Res. **70**:183–232.
5. **Farr GA, Tattersall P.** 2004. A conserved leucine that constricts the pore through the capsid fivefold cylinder plays a central role in parvoviral infection. Virology **323**:243–256.
6. **Fiandra L, Casartelli M, Giordana B.** 2006. The paracellular pathway in the lepidopteran larval midgut: modulation by intracellular mediators. Comp. Biochem. Physiol. A Mol. Comp. Integr. Physiol. **144**:464–473.
7. **Hueffer K, Govindasamy L, Agbandje-McKenna M, Parrish CR.** 2003. Combinations of two capsid regions controlling canine host range determine canine transferrin receptor binding by canine and feline parvoviruses. J. Virol. **77**:10099–10105.
8. **Hueffer K, Parrish CR.** 2003. Parvovirus host range, cell tropism and evolution. Curr. Opin. Microbiol. **6**:392–398.
9. **Jourdan M, et al.** 1990. Cloning of the genome of a densovirus and rescue of infectious virions from recombinant plasmid in the insect host Spodoptera littoralis. Virology **179**:403–409.
10. **Kontou M.** 2005. Structural determinants of tissue tropism and in vivo pathogenicity for the parvovirus minute virus of mice. J. Virol. **79**:10931–10943.
11. **Li Y, et al.** 2001. Genome organization of the densovirus from Bombyx mori (BmDNV-1) and enzyme activity of its capsid. J. Gen. Virol. **82**: 2821–2825.
12. **Mutuel D, et al.** 2010. Pathogenesis of Junonia coenia densovirus in Spodoptera frugiperda: a route of infection that leads to hypoxia. Virology **403**:137–144.
13. **Simpson AA, Chipman PR, Baker TS, Tijssen P, Rossmann MG.** 1998. The structure of an insect parvovirus (Galleria mellonella densovirus) at 3.7 Å resolution. Structure **6**:1355–1367.
14. **Tattersall P, Bergoin M, Bloom ME.** 2005. Parvoviridae, p 353–369. *In* Fauquet CM, et al (ed), Virus taxonomy: VIIIth report of the International Committee on Taxonomy of Viruses. Elsevier/Academic Press, London, United Kingdom.
15. **Ussing HH, Zerahn K.** 1951. Active transport of sodium as the source of electric current in the short-circuited isolated frog skin. Acta Physiol. Scand. **23**:110–127.
16. **Vendeville A, et al.** 2009. Densovirus infectious pathway requires clathrin-mediated endocytosis followed by trafficking to the nucleus. J. Virol. **83**:4678–4689.